assignments for this molecule are consistent with those for ketene imine, thus providing further evidence for the assignments we have made for ketene imine.

Acknowledgment. G.Y.M. thanks the Iraqi Government for a scholarship, and Dr J. August is gratefully thanked for outlining the subtleties of the preparation of ketene imine. The work carried out at the University of Florida was supported by the U.S. Air Force Office of Scientific Research, Division of Chemistry and Atmospheric Sciences, under Contract No. AFOSR-89-0207.

Note Added in Proof. Wentrup et al.[46] have recently detected the elusive ethynamines $HC\equiv CNH_2$ and $PhC\equiv CNH_2$.

(46) Wentrup, C.; Briehl, H.; Lorenčak, P.; Vogelbacher, U. J.; Winter, H.-W.; Maquestiau, A.; Flammung, R. J. Am. Chem. Soc. 1988, 110, 1337.

A Helical Face-Sharing Tetrahedron Chain with Irrational Twist, Stella Quadrangula, and Related Matters

Chong Zheng,[†] Roald Hoffmann,[*,†] and David R. Nelson[‡]

Contribution from the Department of Chemistry and Materials Science Center, Cornell University, Ithaca, New York 14853, and the Lyman Laboratory of Physics, Harvard University, Cambridge, Massachusetts 02138. Received May 19, 1989

Abstract: Aggregates in which tetrahedra share faces are rare; this paper describes the electronic structure of some one-dimensional chains of this type. The archetype is gracefully winding triple helix with irrational twist, also described by R. Buckminster Fuller as a tetrahelix. We examine some realizations of this structure exemplified by stoichiometries such as BR, PtCO, CuI, and TaI. Optimum electron counts for approaching stability in this structural type are given. A related tetracapped tetrahedral building block, the stella quadrangula or tetraederstern, is also the subject of calculations. Undeformed, it cannot propagate in space, but a relatively small distortion of all tetrahedra leads to a reasonably common stacking unit.

Tetrahedra are a ubiquitous building brick of extended one-dimensional structures.[1] Corner-sharing tetrahedral chains of type AX_3, 1, are found in many silicates such as enstatite, jadeite,
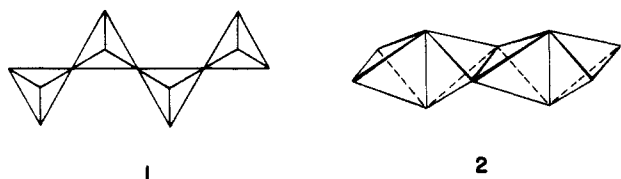

and spodumene.[2] The chain can be linear or helical (e.g. $NaPO_3$).[3] A transition-metal analogue includes K_2CuCl_3.[4] Examples of edge-sharing chains, 2, are $KFeS_2$[5] and K_2PtS_2.[6] Still other types of tetrahedral chains include the corner-connected Rh_4 or Ru_4 tetrahedra in the ternary superconducting borides REM_4B_4.[7]

Face-sharing tetrahedral chains, however, are rare. The isolated $Cu_3I_4^-$ chain in RCu_3I_4 (R = organic counterion) contains a building block made up of three face-sharing tetrahedra. But these blocks are connected by sharing a tetrahedral edge, 3.[8] The basic structural component in RCu_2I_3 is an isolated $Cu_2I_3^-$ unit of two face-sharing tetrahedra, 4.[8,9a] In $[(CoCp_2)(CuI_2)]_3$ there are units consisting of three face-sharing CuI_4 tetrahedra.[9b] Recently, there have been reports of $[Cu_5I_7]^{2-}$ and $[Cu_5Br_7]^{2-}$ chains, in which there are no less than five face-sharing tetrahedra.
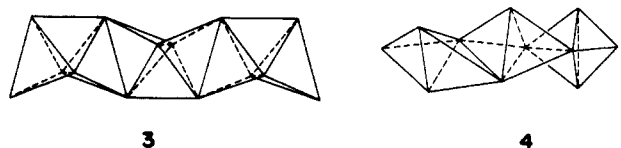
Still another set of molecules with face-sharing tetrahedra as units is to be found in the cluster carbonyls. $Os_5(CO)_{16}$,[10] 5, can

be viewed as two tetrahedra sharing a face, and $Os_6(CO)_{18}$,[11] 6, is a bicapped tetrahedron, or a "chain" of three tetrahedra sharing faces. These tetrahedra are not centered by a metal atom.
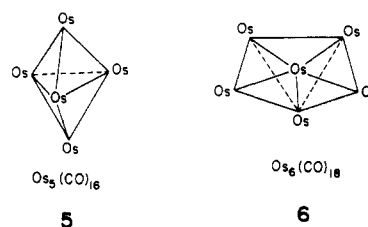
(1) Wells, A. F. Structural Inorganic Chemistry, 4th ed.; Clarendon Press: Oxford, 1975; p 161.
(2) Reference 1, p 817.
(3) Jost, K. H. Acta Crystallogr. 1961, 14, 844.
(4) Brink, C,; Kroese, H. A. S. Acta Crystallogr. 1952, 5, 433. Brink, C.; van Arkel, A. E. Acta Crystallogr. 1952, 5, 506.
(5) (a) Boon, J. W.; MacGillavry, C. H. Recl. Trav. Chim. Pays-Bas 1942, 61, 910. (b) Bronger, W.; Müller, P. J. Less-Common Met. 1984, 100, 241.
(6) Bronger, W.; Günther, O. J. Less-Common Met. 1972, 27, 73.
(7) (a) Matthias, B. T.; Corenzwit, E.; Vandenberg, J. M.; Barz, H. E. Proc. Natl. Acad. Sci. U.S.A. 1977, 74, 1334. (b) Vandenberg, J. M.; Matthias, B. T. Proc. Natl. Acad. Sci. U.S.A. 1977, 74, 1336. (c) Woolf, L. D.; Johnston, D. C.; Mackay, H. B.; McCallum, R. W.; Maple, M. B. J. Low Temp. Phys. 1979, 35, 651. (d) Hornig, H. E.; Shelton, R. N. In Ternary Superconductors; Shenoy, G. K., Dunlap, B. D., Fradin, F. Y., Eds.; North-Holland: New York, 1981; p 213.
(8) Hartl, H.; Mahdjour-Hassan-Abadi, F. Z. Naturforsch. 1984, 39B, 149; Angew. Chem. 1981, 93, 804.
(9) (a) Andersson, S.; Jagner, S. Acta. Chem. Scand. 1985, A39, 181. (b) Hartl, H. Angew. Chem. 1987, 99, 925. (c) Hartl, H.; Mahdjour-Hassan-Abadi, F. Angew. Chem. 1984, 96, 359. Andersson, S.; Jagner, S. J. Crystallogr. Spectroscop. Res. 1988, 18, 601.
(10) (a) Johnson, B. F. G.; Eady, C. R.; Lewis, J.; Reichert, B. E.; Sheldrick, G. M. J. Chem. Soc., Chem. Commun. 1976, 271. (b) Reichert, B. E.; Guy, J. J.; Sheldrick, G. M. Acta Crystallogr. 1977, B33, 173.
(11) (a) Mason, R.; Thomas, K. M.; Mingos, D. M. P. J. Am. Chem. Soc. 1973, 95, 3802. (b) Eady, C. R.; Johnson, B. F. G.; Lewis, J. J. Chem. Soc., Dalton 1975, 2606.

†Cornell University.
‡Harvard University.
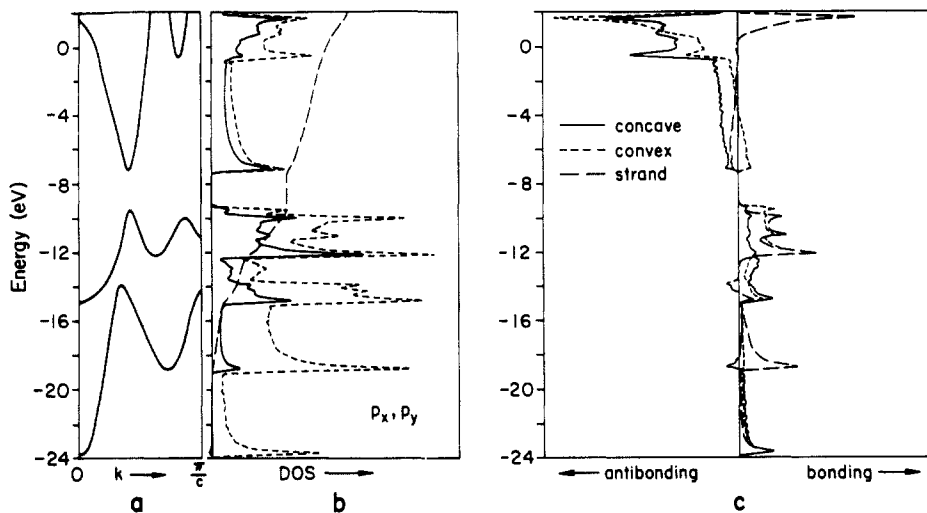
a   b   c

Figure 1. (a) Band structure, (b) density of states (DOS), and (c) crystal orbital overlap population (COOP) for a BH tetrahedral chain. The solid DOS curve shows contributions of p_x and p_y states on B. The dashed and the dotted curves are the integrated and total DOS.

The infinite chain of face-sharing tetrahedra, centered or not, is unknown. The potential existence of such polymers, especially in a remarkable, helical form that we describe in the next section, is the subject of this paper.

Geometrical Aspects

A face-sharing chain of tetrahedra can be built up by adding units one at a time, 7. There is one "dimer" of two tetrahedra, with the symmetry of a trigonal bipyramid, and one trimer, a

7
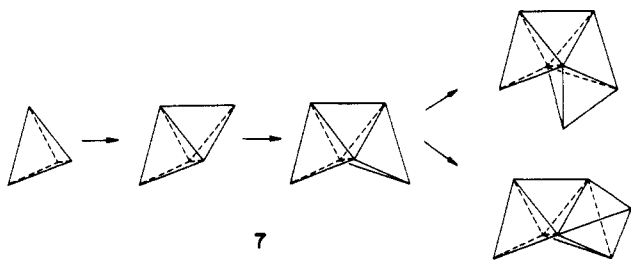
bicapped tetrahedron. On adding further units the number of possible arrangements grows rapidly—there are two tetramers (the first tetramer in 7 is represented by $Cu_5Br_7{}^{2-}$ [9b]), five pentamers, etc. Of the infinite number of structural possibilities of an infinitely extended chain, one has a striking configuration. This is the gracefully winding helix 8.


8
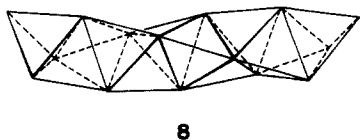
The geometry of a helix is best defined by its unit twist θ and unit height c.[12] The unit twist is the dihedral angle between vectors perpendicularly connecting the successive units and the helix axis (see 9).

9
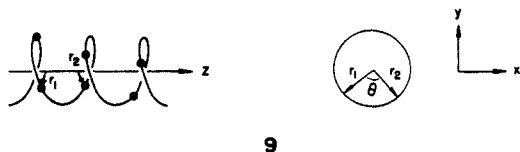
There are two ways to describe this helical structure. In the simplest way we take *one* vertex of a tetrahedron as the helical unit. Then the coordinates of other units can be generated through

$X_n = a\cos{(n\theta)}$, $Y_n = a\sin{(n\theta)}$, $Z_n = nc$, where a and c are 0.5196 and 0.3162 of the tetrahedral edge, respectively (see 10a). In the second description, the helix can be closely associated with a trigonal prismatic structure that we will discuss later. The helical unit is now composed of *three* vertices of a tetrahedron, and the

a

b

10
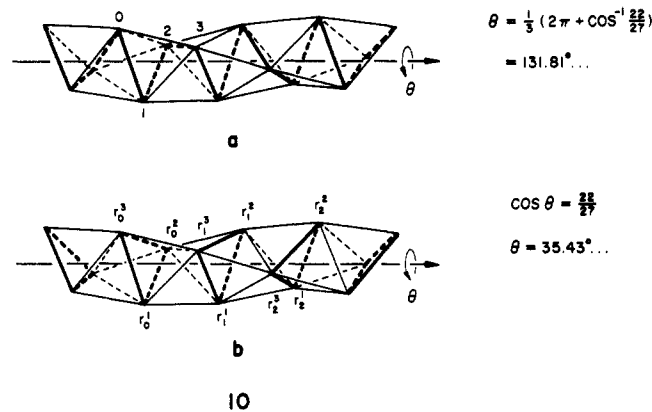
coordinates of all other units can be generated through $X_n^i = a\cos{(n\theta)}$, $Y_n^i = a\sin{(n\theta)}$, $Z_n^i = nc$ ($c = 0.9487$ of the tetrahedral edge, see 10b). The twist of either 10a or 10b is irrational.[13]

Since the twist of 8 is irrational,[13] the helix never repeats itself, so to speak. The translational unit cell is infinite. This establishes a connection to the currently active field of quasiperiodic structures. The lack of a finite translational unit cell might seem at first to pose a problem to the calculation of its electronic structure. But this is not so; the Bloch theorem still applies when translation is accompanied by a rotation.[14] The only difference is that in a band the orbital phase change on going from one unit to another is induced not only by translation but also by rotation. This will become clear in the next section. The tetrahedral helix is also called the "Bernal spiral" in association with discussions of liquid structures in the physics literature.[15]
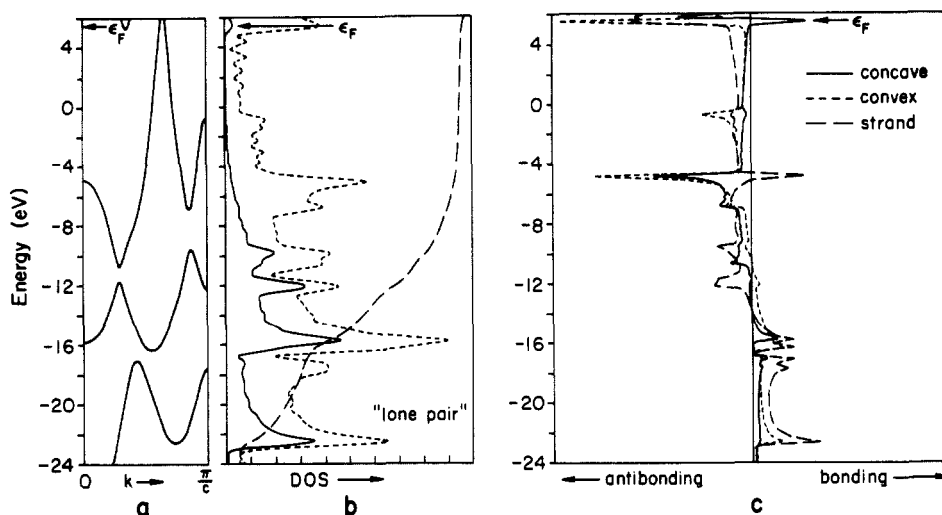
It may be noted at this point that the lovely spiral of tetrahedra has been independently discovered by artists. Buckminster Fuller

---

(12) IUPAC-IUB Commission on Biochemical Nomenclature, 1970. For a brief introduction to helical organic polymers see: Vogl, O.; Jaycox, G. D. *Polymer* **1987**, *28*, 2179.

(13) Coxeter, H. S. M. *Introduction to Geometry*; Wiley: New York, 1969; p 412. See also: Boerdijk, A. H. *Phillips Res. Rep.* **1952**, *7*, 303.

(14) The only requirement is that the group is Abelian and thus can be represented by Bloch waves {e^{ikr}}. In one dimension the group at hand is Abelian, but not in higher dimensions. See: (a) Ashcroft, N. W.; Mermin, N. D. *Solid State Physics*; Sauders College: Philadelphia, 1976. (b) Lax, M. *Symmetry Principles in Solid State and Molecular Physics*; John Wiley & Sons: New York, 1974.

(15) (a) Bernal, J. D. *Proc. R. Soc. London Ser. A* **1964**, *280*, 299. (b) Steinhardt, P. J.; Nelson, D. R.; Ronchetti, M. *Phys. Rev. Lett.* **1981**, *47*, 1297; *Phys. Rev. B* **1983**, *28*, 784. (c) Nelson, D. R. *Phys. Rev. B* **1983**, *28*, 5515.

Figure 2. (a) Band structure, (b) density of states (DOS), and (c) crystal orbital overlap population (COOP) for a tetrahedral chain of S, S–S = 2.1 Å. The DOS (solid line) shows the contribution of an S lone pair, pointing out from the helix. The dotted and dashed lines are the integrated and total DOS.

calls it a tetrahelix[16a] and there is a public sculpture showing the packing of three tetrahelices.[16b]

Realizations of the Helix

We want to be able to specify the most favorable circumstances, geometrical and electronic, for the possible existence of the helical chain, **8**. We will proceed by the construction of some model structures, and carry out for these extended Hückel band calculations, looking for favorable electron counts and bonding patterns. The details of the calculations are given in the Appendix.

We begin with an uncentered tetrahedral chain in which we put a BH at each vertex. We choose BH because (a) the structure is highly triangulated (six triangles meet at each vertex) and boron likes triangles and (b) if we were just to take a B atom, it would be very "exposed" on the outside. The B–B distance we choose is 1.8 Å.

Figure 1 shows the band structure, density of states (DOS), and crystal orbital overlap population (COOP) curve for this polymer. Note that in the helix symmetry there is only one BH per unit cell, so there are few bands. The lowest band is mainly B 2s, and the next band is a mixture of B 2p (and some 2s) and H 1s.

The band structure is very different from other one-dimensional s and p bands we or the reader are likely to have seen. The lowest band (B 2s), for example, goes up, then down, then up again. This is because the unit cell has the same overlap with the next three cells (vertex 0 with vertices 1, 2, and 3 in **10a**). At $k = (1/3)(\pi/c)$, the Bloch phase factors for vertices 1, 2, and 3 are $e^{i\pi/3}$, $e^{i2\pi/3}$, and $e^{i\pi}$, respectively. The bond orders between vertices 0 and 1, 2, 3 are $^1/_2$, $-^1/_2$, and -1, respectively. The total bond order is -1. At $k = (2/3)(\pi/c)$, the individual bond order is $-^1/_2$, $-^1/_2$, and 1, and the total is 0. At $k = \pi/c$, they are -1, 1, and -1 and the total is -1. Thus the B 2s band has two minima at $k = 0$ and $(2/3)(\pi/c)$ (bond orders 3 and 0) and two maxima at $k = (1/3)(\pi/c)$ and π/c (bond orders -1 and -1). For p_z type overlap, the band shape is inverted, like the third band in Figure 1a.

The states immediately above the energy gap around -8 eV are mostly p_x and p_y (x, y perpendicular to helix) states. They are mainly B–B weak antibonding (see Figure 1, a and b) and thus can be identified as π^* type states. Still higher in energy are the states involving B–H antibonding.

The band structure shows that there is a nice gap for two bands filled, i.e. 4 electrons per BH. At the same Fermi level, ca. -9.5 eV, there is maximum B–B and B–H bonding. This may be seen

in the COOP curve. There are actually three distinct pairs of B–B bonds, which we may define as concave edge A, convex edge B, and "strand" edge C, as shown in **11**. The computed overlap populations for the neutral BH polymer are shown in **12**. Note that the concave edge bond is quite a bit weaker than the other two bond types. For comparison the B–B overlap population in octahedral $B_6H_6^{2-}$ (four triangles at each boron) is 0.554, and in icosahedral $B_{12}H_{12}^{2-}$ it is 0.483.
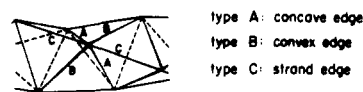
11
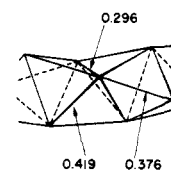
12

One might have imagined that another realization of the helix might be with main group elements (e.g. P or S) bearing a lone pair pointing away, perpendicular to the helix axis. We calculated a hypothetical sulfur case, S–S = 2.1 Å. The band structure, DOS, and COOP curves are shown in Figure 2. Sulfur has 6 electrons and three bands should be filled. The Fermi level is high (5.5 eV) and many S–S antibonding states are filled (see Figure 2c). It is energetically very costly for sulfur to adopt this structure. In fact, triangulated structures are not common for S. Two-connected structures, including helices, are the norm for this element. Note that there are a lot of low-lying "lone pair" states. The "lone pairs" point outward from the vertex; they were used to form B–H bonds in the borane helix. Since there is no ligand to interact with, the "lone pair" states remain more or less localized. Finally, the overlap populations for type A, B, and C bonds are all negative: -0.225, -0.353, and -0.231.

The isolobal analogy[17] allows one to move from main group to transition-metal chemistry. Since $Os(CO)_3$ is isolobal to CH^+ or BH, we may anticipate that an $Os(CO)_3$ tetrahedral chain also has a similar electronic structure. The carbonyls make this structure awfully crowded, so we did not check this by a calculation

(16) (a) Buckminster Fuller, R. *Synergetics*; Macmillan: New York, 1975; pp 513–552. (b) The sculpture, "Triad", is by Ted Bieler. It stands in front of the Marathon Realty Building, University and Front Streets, Toronto. For a photograph of the work see: Lechtman, B. *Photo Life (Canada)* **1987**, July, 15.

(17) (a) Hoffmann, R. *Angew. Chem.* **1982**, *94*, 725; *Angew. Chem., Int. Ed. Engl.* **1982**, *21*, 711. (b) Mingos, D. M. P. *Nature (London) Phys. Sci.* **1972**, *236*, 99. (c) Forsyth, M. I.; Mingos, D. M. P. *J. Chem. Soc., Dalton Trans.* **1977**, 610. (d) Evans, D. G.; Mingos, D. M. P. *Organometallics* **1983**, *2*, 435. (e) Mingos, D. M. P. *Chem. Commun.* **1983**, 706.

A Helical Face-Sharing Tetrahedron Chain

J. Am. Chem. Soc., Vol. 112, No. 10, 1990 3787

but instead tried another metal chain.

## A PtL Tetrahedral Chain and Interconversions of Trigonal Prismatic and Face-Sharing Tetrahedral Structures

Platinum shows a remarkable tendency to form triangulated chains of the $[Pt_3(CO)_6]_n^{2-}$ type, n = 2, 3, 5, 6, 10.[18] These contain a characteristic $Pt_3(CO)_6$ unit, **13**. These triangles are

13

$(Pt_3(CO)_6)_5^{2-}$

14
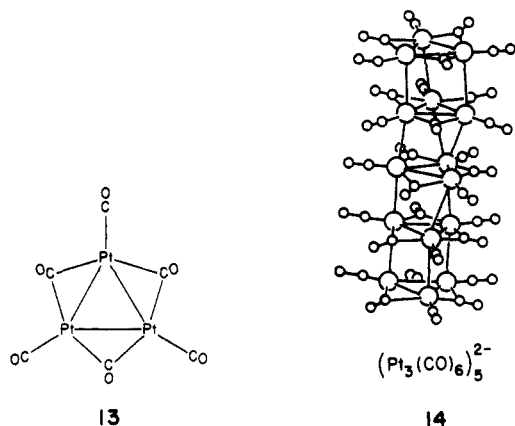
then stacked forming trigonal prisms, antiprisms, and helical structures. For instance the pentamer **14** forms an irregular helix in the solid state, the twist from top to bottom being 64°.

Even two ligands per metal atom leads to steric troubles in the tetrahedral chain. So we were led to a PtL trial geometry, analogous to BH, but with Pt instead of B and CO instead of H.

We also noted that it is possible to deform a perfect trigonal prismatic chain to the tetrahedral one by a continuous transformation defined in **15**. Each chain vertex gains two nearest neighbors in the course of this deformation.

$\theta = 35.43$

$\omega = 50.77$

15
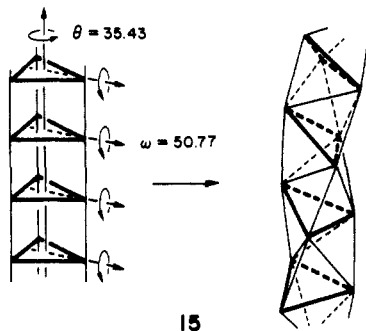
It is instructive to study both the trigonal prismatic and the tetrahedral chain, because we know something about the former, and it gives us an alternative structure to compare.

The electronic structure of the triangular (PtCO)₃ unit has been extensively studied.[19] The d block consists of 15 orbitals (see **16**). Above these d orbitals is an orbital of a_1' symmetry, mainly of Pt s character. There are five degenerate sets in the d block, three of e' and two of e" symmetry. The two e" sets, which are

(18) (a) For a review of large metal clusters see: Chini, P. *J. Organomet. Chem.* **1980**, *200*, 37. (b) Calabrese, J. C.; Dahl, L. F.; Cavalieri, A.; Chini, P.; Longoni, G.; Martinengo, S. *J. Am. Chem. Soc.* **1974**, *96*, 2614. (c) Longoni, G.; Chini, P. *J. Am. Chem. Soc.* **1976**, *98*, 7225. (d) For a recent review of platinum carbonyls see: Clark, H. C.; Jain, V. K. *Coord. Chem. Rev.* **1984**, *55*, 151.

(19) (a) Cotton, F. A.; Haas, T. E. *Inorg. Chem.* **1964**, *3*, 10. (b) Wei, C. H.; Dahl, L. F. *J. Am. Chem. Soc.* **1968**, *90*, 3960. (c) Ruff, J. K.; White, R. P., Jr.; Dahl, L. F. *Ibid.* **1971**, *93*, 2159. (d) Lauher, J. W. *Ibid.* **1978**, *100*, 5305. (e) Dedieu, A.; Hoffmann, R. *Ibid.* **1978**, *100*, 2074. (f) Schilling, B. E. R.; Hoffmann, R. *Ibid.* **1979**, *101*, 3456. (g) Evans, D. G.; Mingos, D. M. P. *Organometallics* **1983**, *2*, 435. (h) Delley, B.; Manning, M. C.; Ellis, D. E.; Berkowitz, J.; Trogler, W. C. *Inorg. Chem.* **1982**, *21*, 2247. (i) Rives, A. B.; Xiao-Zeng, Y.; Fenske, R. F. *Ibid.* **1982**, *21*, 2286. (j) Pacchioni, G.; Fantucci, D.; Valenti, V. *J. Organomet. Chem.* **1982**, *224*, 89. (k) Fantucci, P.; Pacchioni, G.; Valenti, V. *Inorg. Chem.* **1984**, *23*, 247. (l) Chang, K. W.; Woolley, R. G. *J. Phys. C: Solid State Phys.* **1979**, *12*, 2745. (m) Bullett, D. W. *Chem. Phys. Lett.* **1985**, *115*, 450. (n) Mealli, C. *J. Am. Chem. Soc.* **1985**, *107*, 2245. (o) Underwood, D. J.; Hoffmann, R.; Tatsumi, K.; Nakamura, A.; Yamamoto, Y. *J. Am. Chem. Soc.* **1985**, *107*, 5968.
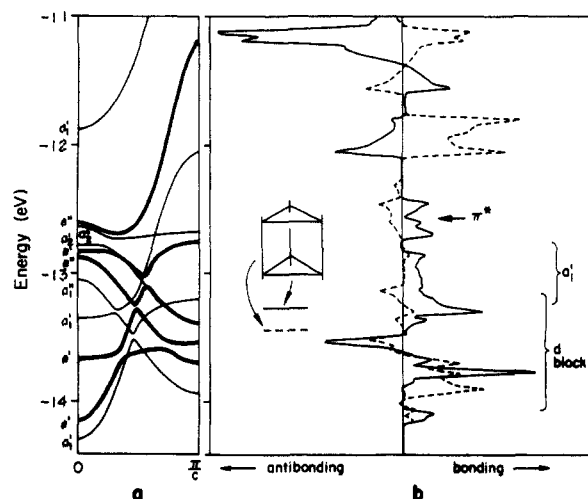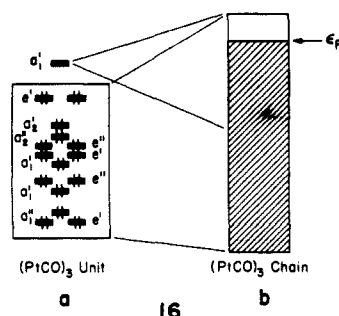

Figure 3. (a) Band structure and (b) COOP of a trigonal prismatic (PtCO)₃ chain.

antisymmetric with respect to the molecular plane, are combinations of xz and yz orbitals.

(PtCO)₃ Unit   (PtCO)₃ Chain

16

When the (PtCO)₃ units are assembled to form the triangular chain, each orbital develops into a band, **16**. The band structure, represented schematically by **16b**, is shown in Figure 3. The intercell interaction rearranges the energy ordering. Away from the Γ point (k = 0, D_{3h} symmetry), the symmetry plane perpendicular to the chain is lost. a', a" (and e', e") bands have avoided crossings.[21] a', e', which are topologically equivalent to an s band, go up; a", e", equivalent to a p_z (z is the chain axis) band, runs downwards. One would expect that the top of the d block is of Pt-Pt antibonding character and the bottom bonding. In reality, the bottom of the metal s,p band mixes in with the top of the d band, making it weakly antibonding or nonbondng.

Also shown in Figure 6 are the COOP curves[20] for the two types of Pt-Pt bonds. In the d block region the states are mostly Pt-Pt bonding except some around -13 eV. The a_1' band, which penetrates into the top of the d block, is also Pt-Pt bonding (see Figure 3b). From the top of the a_1' band begin the CO π* states. Thus an optimal electron count corresponds to the filling of all the d states plus a fraction of the a_1' band. This corresponds to a slightly negatively charged polymer. The overlap populations for the intra- and intercell Pt-Pt are shown in **17**, for a neutral chain (60 electrons per [PtCO]₃). The intracell bond remains stronger for electron counts 60-63 per [Pt(CO)]₃. (Counting 10 electrons from each CO. The *valence* electron count for the neutral fragment is 36, since each CO contributes 2.)

0.168

0.155

17
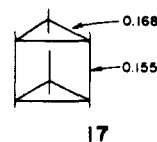
(20) Some other applications of the COOP curves may be found in the following: (a) Wijeyesekera, S. D.; Hoffmann, R. *Organometallics* **1984**, *3*, 949. (b) Kertesz, M.; Hoffmann, R. *J. Am. Chem. Soc.* **1984**, *106*, 3453. (c) Saillard, J.-Y.; Hoffmann, R. *J. Am. Chem. Soc.* **1984**, *106*, 2006.
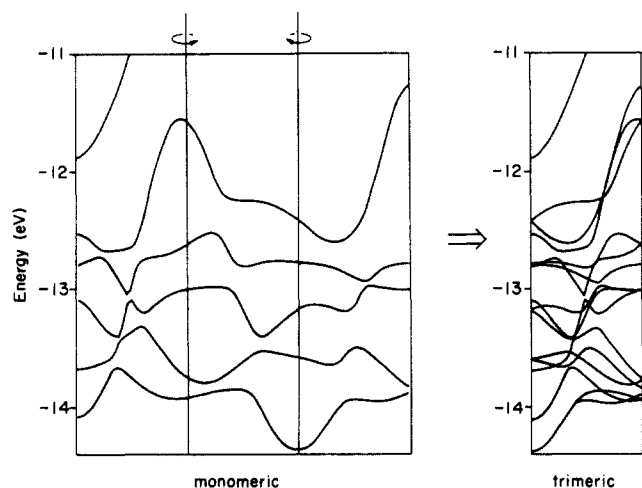
Figure 4. The band structure of a tetrahedral face-sharing chain of PtCO, one formula unit per cell (left), folded back to a trimeric cell (right).
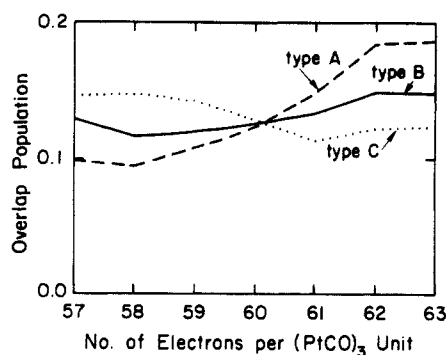
Figure 5. Overlap populations as a function of electron count for the tetrahedral PtCO chain. The three bond types are defined in 11.

Since there is a topological relationship between the trigonal prismatic and the tetrahedral chain, one might expect a similarity between their band structures. To reveal that we have to take the computed band structure for the primitive helical cell of Pt(CO) and fold it back[21] to a trimeric unit, [Pt(CO)]$_3$. This is done in Figure 4. The resemblance to Figure 3 may be seen; the lower symmetry of the tetrahedral chain breaks the degeneracy of the e bands, but otherwise many of the topological features of the triangular band structure are in tact. The overlap populations for a neutral chain, **18**, indicate that the bond strengths are approximately equal. The topological flexibility of the d orbitals
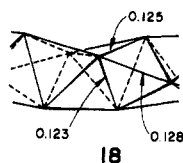
reduces the bond length difference (caused by the strain of the bond angles) that we saw for the borane case. However, away from the neutral chain, the difference in bond strengths becomes larger, as indicated by the overlap populations as a function of the electron count in Figure 5.

The total energy of the tetrahedron chain is lower than that of the triangular chain by an average of ~0.7 eV for 56–63 electrons per (PtCO)$_3$ unit. For neutral PtCO the energy decreases monotonically with twist angle. Though we did not mention it earlier, we also studied a trigonal prismatic BH chain, to compare with the tetrahedral chain in the main group case. The tetrahedral

(21) (a) Hoffmann, R. *Angew. Chem.* **1987**, *99*, 871; *Angew. Chem., Int. Ed. Engl.* **1987**, *26*, 846. (b) Burdett, J. K. *Prog. Solid State Chem.* **1984**, *15*, 173.

chain is also more stable there for the neutral case.

We might mention also that we studied an alternative twisting, now that of alternate Pt$_3$(CO)$_6$ units, thus moving from a trigonal prismatic to an octahedral geometry. The Pt–Pt distance was kept constant at 2.85 Å. The purpose of this was to gain some confidence into the energetics of these angular deformations. Small twists (for instance an average of 16° in the pentamer[18]) are known for the oligomers. The computations give a shallow minimum around 10° twist from the trigonal prism. For a more detailed analysis of these fascinating structures the reader is referred to ref 19o.

MX Tetrahedral Chain

A metal-centered face-sharing tetrahedral chain, **19**, entails a very constrained geometry. The stoichiometry would be MX, and the bond length ratio M–M/M–X = 2/3 for a perfect tetrahedron. For a rather short metal–metal separation of 2.4 Å,

this would require an M–X distance of 3.6 Å. This is too long, even for large ligands of the iodide type. Conversely a typical M–X distance of <3 Å would require unacceptably short metal–metal separations, shorter than the strong quadruply bonded record-short metal–metal bonds we have.

How does one then achieve the "short runs" of face-shared tetrahedra that we saw in the copper iodides mentioned in the introduction? The tetrahedra distort, so as to allow longer metal–metal contacts, near 2.5 Å for Cu(I)–Cu(I). Still another distortion occurs in the many structures that contain the "stella quadrangula" or "tetraederstern" building block, which we will discuss in the next section.

While an undistorted infinite chain of metal-centered face-sharing tetrahedra is unlikely, let us nevertheless see what might be the optimum electron counts for realizing such a geometrical structure. We did calculations for two metal iodides, CuI and TaI. Iodide was chosen because of its large radius, Cu because the structures known contain that metal, and Ta because metal–metal bonding is prevalent around its part of the periodic table.

Figure 6 shows the COOP curves for CuI and TaI helices. The Cu–Cu and Ta–Ta distances are 2.2 and 2.4 Å; thus, Cu–I and Ta–I are 3.3 and 3.6 Å, respectively. For such short metal–metal and long metal–ligand distances, the electronic structure of the materials is dominated by metal–metal bonding. Thus the optimal electron count is such that the d band is a little more than half filled (a little more than half because the bottom of the s, p mixes with the d band). The COOP curves indicate that taking electrons out of CuI or adding electrons to TaI would stabilize the structure.

The Flattened Stella Quadrangula or Tetraederstern Chain

The tetracapped tetrahedron, **20a**, sometimes called stella quadrangula or tetraederstern, is a lovely solid that cannot propagate in space. But a relatively small distortion of all tet-

rahedra results in a flattened D_{2d} unit, **20b**, that readily stacks in one dimension. This structural unit is quite common, and its occurrence in inorganic crystal chemistry has been nicely summarized by Andersson and co-workers.[22]

The one-dimensional chain, **21**, contains two nonequivalent tetrahedral centers, which we can call "i" (inner) and "o" (outer). Many patterns of filling of these tetrahedra can be thought of,

(22) Nyman, H.; Andersson, S. *Acta Crystallogr.* **1979**, *A35*, 580.

A Helical Face-Sharing Tetrahedron Chain

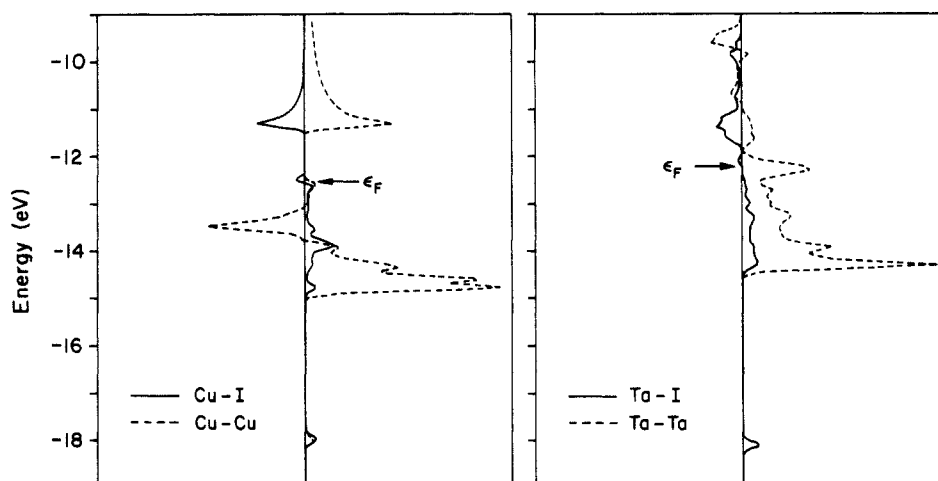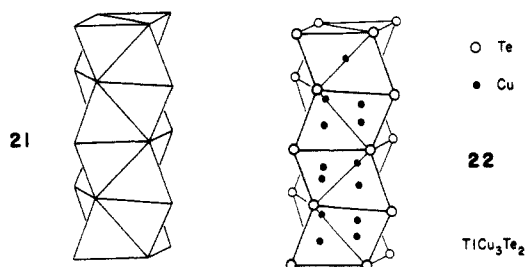*J. Am. Chem. Soc., Vol. 112, No. 10, 1990* 3789

**Figure 6.** Crystal orbital overlap population (COOP) curves for CuI and TaI tetrahedral chains.

and some have been realized. For instance, Klepp and co-workers recently synthesized a compound $TlCu_3Te_2$, **22**, which contains

a linear chain. The building bricks of the chain are the $CuTe_4$ tetrahedrons. The stella quadrangula of Te are alternately filled only in the center tetrahedron and in all the outer ones. The shortest Cu–Cu and Cu–Te contacts are 2.47 and 2.59 Å, respectively.[23]

Since there is no short Te–Te contact in this structure (all Te–Te > 3.95 Å), the formal electron count is $Tl^+Cu_3^{3+}Te_2^{4-}$, giving a d^{10} Cu(I) configuration. The world's record short Cu-(I)–Cu(I) distance is 2.35 Å, which is observed in the linear Cu_3^{3+} chain of a [Cu(tolyl-NNNNN-tolyl]$_3$ complex.[24]

The simple flattening **23**, which changes the tetrahedral angle α from 109.5° to 155.8° while maintaining the M–X distance,

23
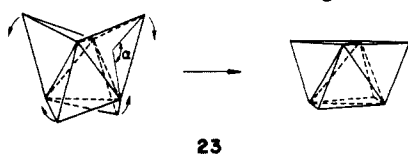
will give a distance ratio $M_i\text{–}M_o/M_i\text{–}M_o'/M\text{–}X/M_o\text{–}M_o/X\text{–}X$ = $1/\sqrt{2}/(3/2)/2\sqrt{(2/3)}/3\sqrt{(2/3)}$ = $1/1.4/1.5/1.6/2.4$. The distance between the inner and outer M sites, $M_i\text{–}M_o$, is that between the centers of two face-sharing tetrahedra. It is very short compared to the next short $M_i\text{–}M_o'$ contact (between the inner M site and the outer M side in another stella quadrangula stacked above or below). Thus there is a geometric constraint preventing both M_i and M_o sites in the same stella quadrangula from being filled simultaneously. The distance $M_o\text{–}M_o'$ between the outer sites of two stacked stella quadragulae is also very short, since it is between the centers of two face-sharing flattened tetrahedra. Unless there is some distortion from the ideal tetrahedral arrangement, the filling of outer sites in two stacked stella quadrangula is unlikely. In Klepp's structure, $TlCu_3Te_2$, the metal tetrahedron formed by the four Cu atoms at the four outer sites shrinks relative to the Te tetrahedra (Cu–Cu = 2.37 → 2.87 Å, Cu–Te = 2.59 → 2.77 Å, whereas the ideal Cu–Cu/Cu–Te is 1.6/1.5, i.e. Cu–Cu is longer than Cu–Te). But each edge of the

(23) Klepp, K. O. *J. Less-Common Met.* **1987**, *128*, 79.
(24) Beck, J.; Strähle, J. *Angew. Chem., Int. Ed. Engl.* **1985**, *24*, 409.

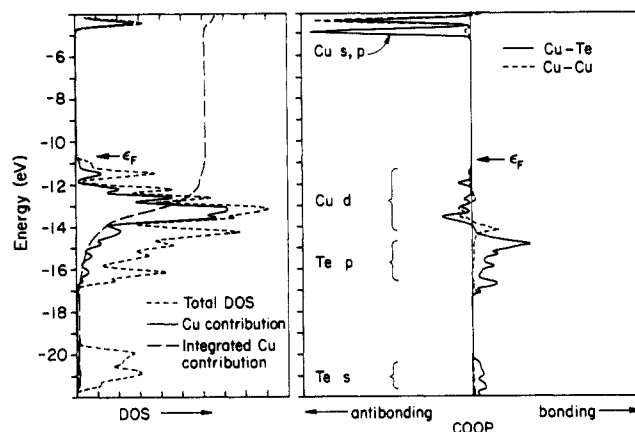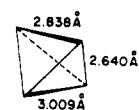**Figure 7.** Density of states (left) and COOP (right) curves for the stella quadrangula chain, $CuTe_2$, in which only the outer sites of every other stella quadrangula are filled.

Table I. Extended-Hückel Parameters

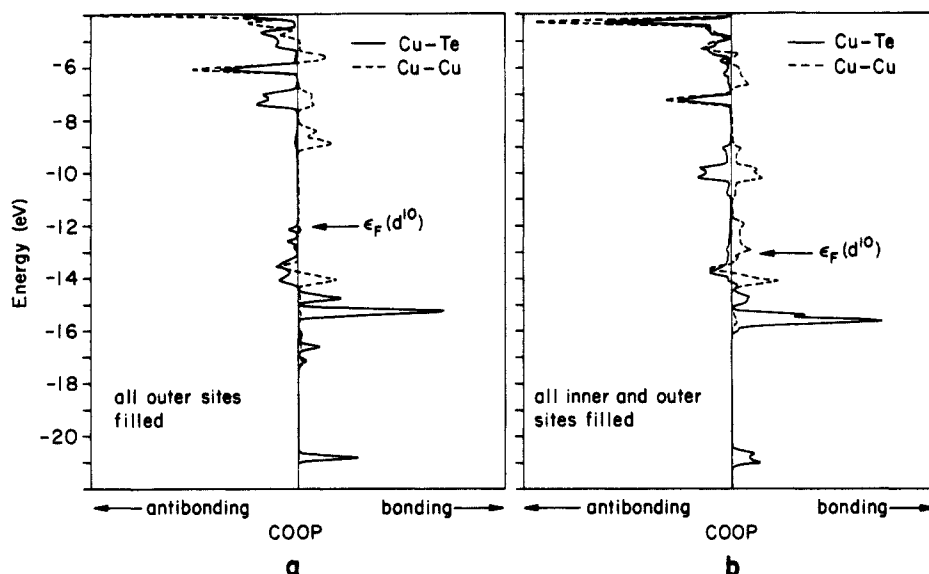| orbital		H_{ii}, eV	$\zeta_1{}^a$	ζ_2	$C_1{}^a$	C_2
H	1s	−13.6	1.3			
B	2s	−15.2	1.3			
	2p	−8.5	1.3			
C	2s	−21.4	1.625			
	2p	−11.4	1.625			
O	2s	−32.3	2.275			
	2p	−14.8	2.275			
S	3s	−20.0	1.82			
	3p	−13.3	1.82			
Te	5s	−20.78	2.51			
	5p	−14.8	2.16			
Pt[19o]	6s	−10.75	2.55			
	6p	−5.27	2.55			
	5d	−13.16	6.01	2.696	0.6332	0.5512
Cu	4s	−11.40	2.20			
	4p	−6.06	2.20			
	3d	−14.00	5.95	2.30	0.5933	0.5744

^{a} Exponents and coefficients in a double-ζ expansion of the d orbitals.

metal tetrahedron shrinks differently, as shown in **24** for one of the tetrahedra (there are two nonequivalent ones in $TlCu_3Te_2$). The top and bottom edges are longer than the side ones. Let us analyze this with our band structure calculation.


24

Figure 8. COOP curves for an expanded copper–tellurium CuTe structure in which (a) all outer sites and (b) all outer and inner sites of each stella quadrangula are filled.

Figure 7 is the DOS and the COOP curve for two representative Cu–Te and Cu–Cu bonds in the one-dimensional stella quadrangula chain (only the outer sites of every other s.q. are filled). Other nonequivalent Cu–Te and Cu–Cu bonds have similar features. In the calculation the Te tetrahedron edge (before the flattening 23) is 4.5 Å, and the Cu tetrahedron is shrunk so that Cu–Cu = 2.6 Å and Cu–Te = 2.68 Å. 25 is a schematic inter-

25
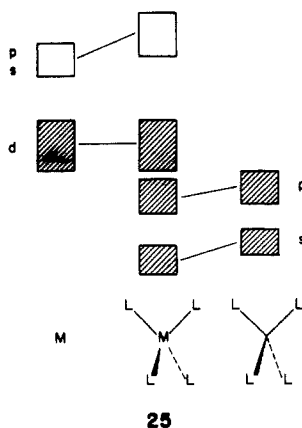
action diagram. The Te(L) s,p blocks are stabilized by Cu(M) d orbitals, the Cu s,p block is pushed up. The Cu d levels are less affected since the destabilization from the orbitals below them is more or less compensated by the orbitals above. From interaction diagram 25, we can easily understand Figure 7. There should be Cu–Te bonding (or nonbonding) in the Cu d and Te p blocks. But the bottom of the Cu d band should be Cu–Cu bonding and the top Cu–Cu weakly antibonding due to the mixing of Cu s,p with the filled d band, such as that shown in 26. The overall Cu–Cu interaction will become attractive, as is the case in many aggregated Cu(I) clusters.


26
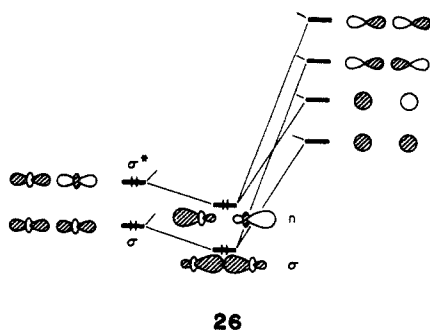
The computed overlap populations for the two nonequivalent Cu–Cu contacts in the stella quadrangula chain (only the outer sites of every other stella quadrangula are filled) are shown in 27. Indeed, the positive values indicate attractive Cu–Cu interactions. As we mentioned before, all Cu–Cu distances in this metal


27
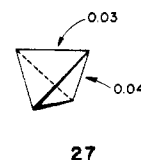
tetrahedron are 2.6 Å. The relative overlap populations are indicative of the observed bond strength in the actual structure; the top and bottom edges are longer than the side edges (see 24).

The differential in the overlap population is partially a consequence of the flattening of the stella quadrangula 23. Four Te atoms at the stella quadrangula corners are aligned closer in height to the Cu atoms (see 28). Thus orbital n in 26, which is slightly


28
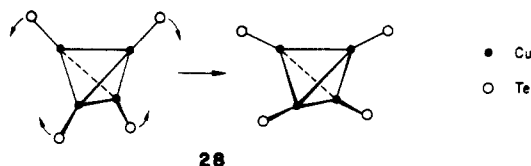
Cu–Cu antibonding, interacts with Te because it points toward the ligands. This is shown in 29.

29
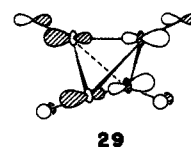
The stabilizing interaction 29 pulls more n states (see 28) down below the Fermi level. Unlike the discrete molecular case, some n states here are above the Fermi level and unfilled because of the band dispersion. The net result is a weakening of the top and bottom edge of the metal tetrahedron. If we decrease the interaction between the four Te atoms and the Cu's by changing the Slater orbital exponent of Te from 2.5 and 2.16 to 3.0, the overlap population will become more or less equal (0.033 vs 0.032). The electron density in Cu p_x, which is a constituent of orbital n, will decrease from 0.17 to 0.10, because less n states are pulled down below the Fermi level.

When the outer and inner sites are alternately filled, another kind of Cu_o–Cu_i bond is formed. It is from the outer Cu to the

inner Cu in an adjacent stella quadrangula and has the same bond length as that within the metal tetrahedron. The calculated overlap populations are shown in **30**. The difference between the top and side bond strengths in the metal tetrahedron is increased. It is because more bonding states for the top edge are pushed up by interactions such as **31**. The bonding σ orbital in **26** has its

30   **31**
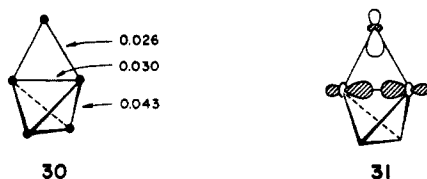
electron density localized at the center of the bond, thus it interacts better with the Cu_I atom than other antibonding orbitals such as n.

We have performed calculations on the stella quadrangula chain in which all inner sites or all outer sites are filled. When only all inner sites are filled, there are not enough M–X bonds to hold the structure from collapsing. If all outer sites are filled, there is the crowding effect between the metal atoms between adjacent stella quadrangula which gives unreasonably large negative overlap population values. The structure seems to be best filled alternatively, unless it expands to relieve the crowding effect. Figure 8 shows the COOP curves for the expanded structure, in which the shortest Cu–Cu and Cu–Te contacts are around 2.6 and 2.7 Å, respectively. Here again, the mixing of the Cu s,p band into the d band has reduced the antibonding feature at the top of the d band. Thus high occupancy of the d band is possible, even for an expanded structure with all outer or all inner and outer sites filled.

In this paper we have fleshed out the beautiful, seductive geometry of a spiral chain of face-sharing tetrahedra, by adducing several molecular realizations. The optimal electron counts for these hypothetical one-dimensional arrays are computed.

Still another, even more speculative potentiality for realizing the tetrahedral chain is to have each tetrahedron centered by a water molecule, with hydrogen bonds piercing the shared tetrahedral faces. Such a helical $(H_2O)_n$ chain would contain alternating nonequivalent water molecules, the chain formed by their O–H bonds and lone pairs. Stacking of such structures could lead to geometries related to the clathrates and gas hydrates.[25]

Appendix

The extended-Hückel method[26] was used in the calculations. The Bloch sum in the helical structure is $\sum_R e^{ik \cdot R} T_R \phi_i$, where ϕ_i is the atomic wave function in the unit cell, T_R is the translation-rotation operator, and k is the Bloch wave vector. The summation is over all cells. The energies and overlap populations are calculated with 100K points along the one-dimensional reciprocal space.

The interatomic distances used are the following: B–H = 1.28 Å, B–B = 1.80 Å,[27] Pt–Pt = 2.85 Å, Pt–C = 2.1 Å, C–O = 1.16 Å.[19] The extended-Hückel parameters are listed in Table I.

(25) These Frank–Kasper structures with rare gas atoms at the vertices are reviewed by: Berecz, E.; Balla-Achs, A. *Gas Hydrates*; Elsevier: Amsterdam, 1983.

(26) Hoffmann, R. *J. Chem. Phys.* **1963,** *39,* 1397. Hoffmann, R.; Lipscomb, W. N. *Ibid.* **1962,** *36,* 2179; *37,* 2872. Ammeter, J. H.; Bürgi, H.-B.; Thibeault, J. C.; Hoffmann, R. *J. Am. Chem. Soc.* **1978,** *100,* 3686. Whangbo, M.-H.; Hoffmann, R.; Woodward, R. B. *Proc. R. Soc. London* **1979,** *A366,* 23.

(27) Lipscomb, W. N. *Boron Hydrides*; Benjamin: New York, 1963.

A Global Approach to Molecular Symmetry: Theorems on Symmetry Relations between Ground- and Excited-State Configurations

Paul G. Mezey

Contribution from the Department of Chemistry and Department of Mathematics, University of Saskatchewan, Saskatoon, Saskatchewan, Canada, S7N 0W0. Received June 6, 1989

Abstract: Several simple rules have been derived, providing new insight into the role of point symmetry in controlling the energetic stability of molecules and excited-state species. General symmetry conditions have been found that interrelate the ground-state and electronic excited-state energy minima, transition structures and other stationary nuclear arrangements of neutral molecules and ions, and excimers and exciplexes. By testing the point symmetry of a family of nuclear arrangements, one can predict the existence of stationary nuclear configurations within domains of a whole series of ground- and excited-state potential energy surfaces. The *catchment region point symmetry theorem* and various *vertical symmetry theorems* provide new tools for the analysis of potential surfaces and a rational strategy for the search for stationary points. The applications of the theorems are illustrated by examples.

The usual question asked when studying molecular symmetry problems is the following: what is the point symmetry group of some specified nuclear configuration? If the point symmetry is determined, then various conclusions can be drawn concerning the properties of the specified molecular species.[1–6]

In this study we shall view the problem from a different perspective and ask different questions: if all possible configurations of a collection of atoms is considered, then which are those configurations that have a specified symmetry? What predictions

(1) McWeeny, R. *Symmetry, An Introduction to Group Theory and Its Applications*; Pergamon Press: New York, 1963.

(2) Tinkham, M. *Group Theory and Quantum Mechanics*; McGraw-Hill: New York, 1964.

(3) Hochstrasser, R. M. *Molecular Aspects of Symmetry*; Benjamin, Inc.: New York, 1966.

(4) Bishop, D. *Group Theory in Chemistry*; Oxford University Press: London, 1973.

(5) Ezra, G. S. *Symmetry Properties of Molecules*; Springer Verlag: Berlin, 1982.

(6) Hargittai, I.; Hargittai, M. *Symmetry through the Eyes of a Chemist*; VCH Publishers: New York, 1986.